

Received 22 May 2024, accepted 12 June 2024, date of publication 17 June 2024, date of current version 24 June 2024.

Digital Object Identifier 10.1109/ACCESS.2024.3415548



Super-Node Approximation With Convex Hulls Relaxation for Distribution System Restoration Using ERRs

SANTOSH SHARMA[®], (Graduate Student Member, IEEE), AND QIFENG LI[®], (Senior Member, IEEE)

Department of Electrical and Computer Engineering, University of Central Florida, Orlando, FL 32816, USA

Corresponding author: Qifeng Li (qifeng.li@ucf.edu)

This work was supported in part by the University of Central Florida (UCF), College of Graduate Studies Open Access Publishing Fund. The work of Qifeng Li was supported by the U.S. National Science Foundation under Awards CBET 2124849 and 2402495.

ABSTRACT Emergency response resources (ERRs) such as mobile energy resources (MERs) and repair crews (RCs) play a pivotal role in the efficient restoration of power distribution systems after disasters. This paper presents a computationally tractable approach to utilize ERRs and post-disaster available distributed energy resources (PDA-DERs) in the restoration of disaster-impacted distribution systems. The post-disaster restoration model is proposed to co-optimize the dispatch of pre-allocated ERRs and PDA-DERs to minimize the impact of high-impact low-frequency (HILF) events on customers, i.e., energy not served for the entire restoration window. Compared with existing restoration strategies using ERRs, the proposed approach is more tractable since, in the restoration model, a super-node approximation (SNA) of distribution networks and the convex hulls relaxation (CHR) of non-linear constraints are introduced to achieve the best trade-off between computational burden and accuracy. Tests of the proposed approach on IEEE test feeders demonstrated that a combination of SNA and CHR remarkably reduces the solution time of the post-disaster restoration model.

INDEX TERMS Distribution system restoration, emergency response resources, convex hulls relaxation, super-node approximation, mobile energy resources.

NOMENCLATU	RE	MESSs	Mobile Energy storage system.
Sets		MICP	Mixed-integer convex program.
$\Omega_{ders},\Omega_{mers}$	Set of DERs, MERs.	MINLP	Mixed-integer non-linear program.
Ω_{res}	Set of MDGs, SDGs and SPVs.	PDA-DERs	Post-disaster available DERs.
Ω_s	Set of MESSs & SESSs.	RCs	Repair crews.
Acronyms		SDGs	Static Diesel/distributed generators.
CHR	Convex hulls relaxation.	SESSs	Static Energy storage systems.
DERs	Distributed energy resources.	SNA	Super-node approximation.
DSO	Distribution system operator.	SPVs	Static Photovoltaics.
ERRs	Emergency response resources.	Parameters	
MDGs	Mobile Diesel Generators.	$\overline{\ell_{ik}}$	Squared of current capacity (thermal)
MERs	Mobile energy resources.		limit of line <i>ik</i> .
		$\overline{p}_{i,t}^{\mathrm{L}}, p_{i,t}^{\mathrm{L}},$	
		$egin{aligned} p_{i,t}^-, & \underline{p}_{i,t}^-, \ \overline{q}_{i,t}^\mathrm{L}, & \underline{q}_{i,t}^\mathrm{L} \end{aligned}$	Maximum and minimum active and
The associate of	editor coordinating the review of this manuscript and	,	reactive power demand at node i at

time t.

approving it for publication was Qiang Li^D.



$\begin{array}{llllllllllllllllllllllllllllllllllll$	\overline{S}_{ik}	Power carrying capacity limit of line ik
RT $_{i,n}$ Travel time between node i and node n . TT $_{j,i,ik}$ Travel time between line ji and line ik . Squared of minimum and maximum limits of voltage at node i . Leghes_spl Initial energy in j th unit of MESSs. $E_{i,j}^{SES_c}$ Capacity (MWh, MVA) of j th unit of SESSs at node i . Leghes_s Sesses at node i . Leghes_s Sesses can ode i . L		
$\begin{array}{llll} \operatorname{TT}_{i,n} & \operatorname{Travel time between node } i \text{ and node } n. \\ \operatorname{TT}_{ji,ik} & \operatorname{Squared of minimum and maximum limits of voltage at node } i. \\ E_{j}^{\operatorname{MES_spl}} & \operatorname{Initial energy in } j \text{th unit of MESSs.} \\ E_{i,j}^{\operatorname{SES_spl}} & \operatorname{Initial energy in } j \text{th unit of SESSs at node } i. \\ E_{i,j}^{\operatorname{SES_spl}} & \operatorname{Size (MWh, MVA) of } j \text{th unit of SESSs at node } i. \\ E_{i,j}^{\operatorname{MES_s}} & \operatorname{Size (MWh, MVA) of } j \text{th unit of MESSs.} \\ E_{i,j}^{\operatorname{MES_s}} & \operatorname{Size (MWh, MVA) of } j \text{th unit of MESSs.} \\ E_{i,j}^{\operatorname{MES_s}} & \operatorname{Size (MWh, MVA) of } j \text{th unit of MESSs.} \\ E_{i,j}^{\operatorname{MES_s}} & \operatorname{Size (MWh, MVA) of } j \text{th unit of MESSs.} \\ E_{i,j}^{\operatorname{MES_s}} & \operatorname{Size (MWh, MVA) of } j \text{th unit of MESSs.} \\ E_{i,j}^{\operatorname{MES_s}} & \operatorname{Size (MWh, MVA) of } j \text{th unit of MESSs.} \\ E_{i,j}^{\operatorname{MES_s}} & \operatorname{Size (MWh, MVA) of } j \text{th unit of MESSs.} \\ E_{i,j}^{\operatorname{MES_s}} & \operatorname{Size (MWh, MVA) of } j \text{th unit of MESSs.} \\ E_{i,j}^{\operatorname{MES_s}} & \operatorname{Number of nodes/super-nodes.} \\ E_{i,j}^{\operatorname{MES_s}} & \operatorname{Number of nodes/super-nodes.} \\ E_{i,j}^{\operatorname{MES_s}} & \operatorname{Number of PDA-DERs (SDGs, SESSs, SPVs) at node } i. \\ E_{i,j}^{\operatorname{MES_s}} & \operatorname{Number of PDA-DERs (SDGs, SESSs, SPVs) at node } i. \\ E_{i,j}^{\operatorname{MES_s}} & \operatorname{Active, reactive power capacity of } j \text{th unit of SDGs at node } i.} \\ E_{i,j}^{\operatorname{G}} & \operatorname{Active power capacity of } j \text{th unit of SPVs at node } i.} \\ E_{i,j}^{\operatorname{G}} & \operatorname{Available active, reactive grid power at node } i \text{ at time } t.} \\ E_{i,j}^{\operatorname{MES_s}} & \operatorname{Size (MW) of } j \text{th unit of MDGs.} \\ E_{i,j}^{\operatorname{ESS_s}} & \operatorname{ExS_s} \\ E_{$	RT_{ij}	
$\begin{array}{lll} \operatorname{TT}_{ji,ik} & \operatorname{Travel time between line } ji \text{ and line } ik. \\ \operatorname{Squared of minimum and maximum limits of voltage at node } i. \\ E_{j}^{\operatorname{MES_spl}} & \operatorname{Initial energy in } jth \text{ unit of MESSs.} \\ E_{i,j}^{\operatorname{SES_c}} & \operatorname{SESS_c} \\ S_{i,j}^{\operatorname{SES_c}} & \operatorname{Capacity (MWh, MVA) of } jth \text{ unit of SESSs at node } i. \\ E_{j}^{\operatorname{MES_s}} & \operatorname{Size (MWh, MVA) of } jth \text{ unit of MESSs.} \\ S_{j}^{\operatorname{MES_s}} & \operatorname{Size (MWh, MVA) of } jth \text{ unit of MESSs.} \\ S_{j}^{\operatorname{MES_s}} & \operatorname{Size (MWh, MVA) of } jth \text{ unit of MESSs.} \\ S_{j}^{\operatorname{MES_s}} & \operatorname{Size (MWh, MVA) of } jth \text{ unit of MESSs.} \\ S_{j}^{\operatorname{MES_s}} & \operatorname{Size (MWh, MVA) of } jth \text{ unit of MESSs.} \\ S_{j}^{\operatorname{MES_s}} & \operatorname{Size (MWh, MVA) of } jth \text{ unit of MESSs.} \\ S_{j}^{\operatorname{MES_s}} & \operatorname{Size (MWh, MVA) of } jth \text{ unit of MESSs.} \\ S_{j}^{\operatorname{MES_s}} & \operatorname{Max} & \operatorname{Max}$		
$\begin{array}{lll} \underline{v_i}, \overline{v_i} & \text{Squared of minimum and maximum limits of voltage at node } i. \\ E_j^{\text{MES_spl}} & \text{Initial energy in } j\text{th unit of MESSs.} \\ E_{i,j}^{\text{SES_cpl}} & \text{Initial energy in } j\text{th unit of SESSs at node } i. \\ E_{i,j}^{\text{SES_c}}, & \\ S_{i,j}^{\text{SES_c}} & \text{Capacity (MWh, MVA) of } j\text{th unit of SESSs at node } i. \\ E_j^{\text{MES_s}}, & \\ S_j^{\text{MES_s}}, & \\ S_$	$TT_{i,n}$	
Ilimits of voltage at node <i>i</i> . EMES_spl JessS_spl Jess		· ·
$E_{j}^{\text{MES_spl}} \qquad \qquad \text{Initial energy in } j \text{th unit of MESSs.} \\ E_{i,j}^{\text{SES_spl}} \qquad \qquad \text{Initial energy in } j \text{th unit of SESSs at node } i. \\ E_{i,j}^{\text{SES_c}} \qquad \qquad \text{Capacity (MWh, MVA) of } j \text{th unit of SESSs at node } i. \\ E_{i,j}^{\text{MES_s}} \qquad \qquad \text{Size (MWh, MVA) of } j \text{th unit of MESSs.} \\ E_{i,j}^{\text{MES_s}} \qquad \qquad \text{Size (MWh, MVA) of } j \text{th unit of MESSs.} \\ E_{i,j}^{\text{MES_s}} \qquad \qquad \text{Size (MWh, MVA) of } j \text{th unit of MESSs.} \\ E_{i,j}^{\text{MES_s}} \qquad \qquad \text{Size (MWh, MVA) of } j \text{th unit of MESSs.} \\ E_{i,j}^{\text{MES_s}} \qquad \qquad \text{Size (MWh, MVA) of } j \text{th unit of MESSs.} \\ \text{MADG, SDGs, and SPVs.} \qquad \qquad \text{A Big-M constant.} \\ \text{Number of nodes/super-nodes.} \\ \text{Number of PDA-DERs (SDGs, SESSs, SPVs) at node } i. \\ \text{Number of PDA-DERs (SDGs, SESSs, SPVs) at node } i. \\ \text{Hourly solar irradiation profile.} \\ \text{Polity} \qquad \qquad \text{Active, reactive power capacity of } j \text{th unit of SDGs at node } i. \\ \text{Active power capacity of } j \text{th unit of SPVs at node } i. \\ \text{Available active, reactive grid power at node } i \text{ at time } t. \\ \text{Size (MW) of } j \text{th unit of MDGs.} \\ \text{Size (MW) of } j \text{th unit of MDGs.} \\ \text{Size (MW) of } j \text{th unit of SESSs at node } i. \\ \text{Resistance and reactance of line } i k. \\ \text{Resistance and reactance of line } i k. \\ \text{Resistance of } j \text{th unit of MESSs.} \\ \text{Total number of available MDGs,} \\ \text{MESSs units.} \\ \text{Total number of RCs allowed to repair a damaged line simultaneously.} \\ \end{array}$	$\frac{v_i}{}$, v_i	
node i . $S_{i,j}^{SES_c}$, $S_{i,j}^{SES_c}$ Capacity (MWh, MVA) of j th unit of SESSs at node i . $E_{i,j}^{MES_s}$, $S_{j}^{MES_s}$ Size (MWh, MVA) of j th unit of MESSs. k_1, k_2 Parameters used to maintain the ratio of active and reactive power outputs of MDGs, SDGs, and SPVs. M A Big-M constant. N Number of nodes/super-nodes. N_{i}^{SDG} , N_{i}^{SES} , N_{i}^{SPV} Number of PDA-DERs (SDGs, SESSs, SPVs) at node i . $P_{i}^{profile}$ Hourly solar irradiation profile. $P_{i,j}^{SDG_c}$ Active, reactive power capacity of j th unit of SDGs at node i . $P_{i,j}^{SPV_c}$ Active power capacity of j th unit of SPVs at node i . $P_{i,j}^{G}$ Available active, reactive grid power at node i at time t . $P_{i,j}^{MDG_s}$ Size (MW) of j th unit of MDGs. $P_{i,j}^{SES_bt}$ Converter + battery, converter, battery resistance of j th unit of SESSs at node i . $P_{i,k}^{MES_e}$, $P_{i,j}^{MES_e}$, P_{i,j	_MES_spl	_
node i . $S_{i,j}^{SES_c}$, $S_{i,j}^{SES_c}$ Capacity (MWh, MVA) of j th unit of SESSs at node i . $E_{i,j}^{MES_s}$, $S_{j}^{MES_s}$ Size (MWh, MVA) of j th unit of MESSs. k_1, k_2 Parameters used to maintain the ratio of active and reactive power outputs of MDGs, SDGs, and SPVs. M A Big-M constant. N Number of nodes/super-nodes. N_{i}^{SDG} , N_{i}^{SES} , N_{i}^{SPV} Number of PDA-DERs (SDGs, SESSs, SPVs) at node i . $P_{i}^{profile}$ Hourly solar irradiation profile. $P_{i,j}^{SDG_c}$ Active, reactive power capacity of j th unit of SDGs at node i . $P_{i,j}^{SPV_c}$ Active power capacity of j th unit of SPVs at node i . $P_{i,j}^{G}$ Available active, reactive grid power at node i at time t . $P_{i,j}^{MDG_s}$ Size (MW) of j th unit of MDGs. $P_{i,j}^{SES_bt}$ Converter + battery, converter, battery resistance of j th unit of SESSs at node i . $P_{i,k}^{MES_e}$, $P_{i,j}^{MES_e}$, P_{i,j	E_{j}^{mass}	Initial energy in jth unit of MESSs.
node i . $S_{i,j}^{SES_c}$, $S_{i,j}^{SES_c}$ Capacity (MWh, MVA) of j th unit of SESSs at node i . $E_{i,j}^{MES_s}$, $S_{j}^{MES_s}$ Size (MWh, MVA) of j th unit of MESSs. k_1, k_2 Parameters used to maintain the ratio of active and reactive power outputs of MDGs, SDGs, and SPVs. M A Big-M constant. N Number of nodes/super-nodes. N_{i}^{SDG} , N_{i}^{SES} , N_{i}^{SPV} Number of PDA-DERs (SDGs, SESSs, SPVs) at node i . $P_{i}^{profile}$ Hourly solar irradiation profile. $P_{i,j}^{SDG_c}$ Active, reactive power capacity of j th unit of SDGs at node i . $P_{i,j}^{SPV_c}$ Active power capacity of j th unit of SPVs at node i . $P_{i,j}^{G}$ Available active, reactive grid power at node i at time t . $P_{i,j}^{MDG_s}$ Size (MW) of j th unit of MDGs. $P_{i,j}^{SES_bt}$ Converter + battery, converter, battery resistance of j th unit of SESSs at node i . $P_{i,k}^{MES_e}$, $P_{i,j}^{MES_e}$, P_{i,j	$E_{i,i}^{SES_spl}$	Initial energy in jth unit of SESSs at
SESSs at node i . $E_j^{\text{MES_s}}$, $S_j^{\text{MES_s}}$ Size (MWh, MVA) of j th unit of MESSs. k_1, k_2 Parameters used to maintain the ratio of active and reactive power outputs of MDGs, SDGs, and SPVs. M A Big-M constant. N Number of nodes/super-nodes. N_i^{SDG} , N_i^{SES} , N_i^{SPV} Number of PDA-DERs (SDGs, SESSs, SPVs) at node i . $p_{i,j}^{\text{SDG_c}}$ Active, reactive power capacity of j th unit of SDGs at node i . $p_{i,j}^{\text{SPV_c}}$ Active power capacity of j th unit of SPVs at node i . $p_{i,j}^{\text{SPV_c}}$ Active power capacity of j th unit of SPVs at node i . $p_{i,j}^{\text{MDG_s}}$ Available active, reactive grid power at node i at time t . $p_{i,j}^{\text{MDG_s}}$ Size (MW) of j th unit of MDGs. $r_{i,j}^{\text{SES_bt}}$ Converter $+$ battery, converter, battery resistance of j th unit of SESSs at node i . r_{ik} , x_{ik} Resistance and reactance of line ik . $r_{ik}^{\text{MES_bt}}$ Converter $+$ battery, converter, battery resistance of j th unit of MESSs. t^{MDG} , t^{MES} Total number of available MDGs, MESSs units. T^{RC} Total number of RCs allowed to repair a damaged line simultaneously.		node i .
SESSs at node i . $E_j^{\text{MES_s}}$, $S_j^{\text{MES_s}}$ Size (MWh, MVA) of j th unit of MESSs. k_1, k_2 Parameters used to maintain the ratio of active and reactive power outputs of MDGs, SDGs, and SPVs. M A Big-M constant. N Number of nodes/super-nodes. N_i^{SDG} , N_i^{SES} , N_i^{SPV} Number of PDA-DERs (SDGs, SESSs, SPVs) at node i . $p_{i,j}^{\text{SDG_c}}$ Active, reactive power capacity of j th unit of SDGs at node i . $p_{i,j}^{\text{SPV_c}}$ Active power capacity of j th unit of SPVs at node i . $p_{i,j}^{\text{SPV_c}}$ Active power capacity of j th unit of SPVs at node i . $p_{i,j}^{\text{MDG_s}}$ Available active, reactive grid power at node i at time t . $p_{i,j}^{\text{MDG_s}}$ Size (MW) of j th unit of MDGs. $r_{i,j}^{\text{SES_bt}}$ Converter $+$ battery, converter, battery resistance of j th unit of SESSs at node i . r_{ik} , x_{ik} Resistance and reactance of line ik . $r_{ik}^{\text{MES_bt}}$ Converter $+$ battery, converter, battery resistance of j th unit of MESSs. t^{MDG} , t^{MES} Total number of available MDGs, MESSs units. T^{RC} Total number of RCs allowed to repair a damaged line simultaneously.	$E_{::}^{SES_c}$,	
SESSs at node i . $E_j^{\text{MES_s}}$, $S_j^{\text{MES_s}}$ Size (MWh, MVA) of j th unit of MESSs. k_1, k_2 Parameters used to maintain the ratio of active and reactive power outputs of MDGs, SDGs, and SPVs. M A Big-M constant. N Number of nodes/super-nodes. N_i^{SDG} , N_i^{SES} , N_i^{SPV} Number of PDA-DERs (SDGs, SESSs, SPVs) at node i . $p_{i,j}^{\text{SDG_c}}$ Active, reactive power capacity of j th unit of SDGs at node i . $p_{i,j}^{\text{SPV_c}}$ Active power capacity of j th unit of SPVs at node i . $p_{i,j}^{\text{SPV_c}}$ Active power capacity of j th unit of SPVs at node i . $p_{i,j}^{\text{MDG_s}}$ Available active, reactive grid power at node i at time t . $p_{i,j}^{\text{MDG_s}}$ Size (MW) of j th unit of MDGs. $r_{i,j}^{\text{SES_bt}}$ Converter $+$ battery, converter, battery resistance of j th unit of SESSs at node i . r_{ik} , x_{ik} Resistance and reactance of line ik . $r_{ik}^{\text{MES_bt}}$ Converter $+$ battery, converter, battery resistance of j th unit of MESSs. t^{MDG} , t^{MES} Total number of available MDGs, MESSs units. T^{RC} Total number of RCs allowed to repair a damaged line simultaneously.	SES_c	Canacity (MWh MVA) of ith unit of
$\begin{array}{lll} E_{j}^{\text{MES_s}}, \\ S_{j}^{\text{MES_s}} & \text{Size (MWh, MVA) of } \textit{jth unit of MESSs.} \\ k_{1}, k_{2} & \text{Parameters used to maintain the ratio} \\ & & \text{of active and reactive power outputs of} \\ & & \text{MDGs, SDGs, and SPVs.} \\ M & & \text{A Big-M constant.} \\ N & & \text{Number of nodes/super-nodes.} \\ N_{j}^{\text{SDG}}, N_{j}^{\text{SES}}, \\ N_{j}^{\text{SPV}} & & \text{Number of PDA-DERs (SDGs, SESSs, SPVs) at node } \textit{i.} \\ p_{i,j}^{\text{profile}} & & \text{Hourly solar irradiation profile.} \\ p_{i,j}^{\text{SDG_c}}, & & \text{Active, reactive power capacity of } \textit{jth unit of SDGs at node } \textit{i.} \\ p_{i,j}^{\text{SPV_c}} & & \text{Active power capacity of } \textit{jth unit of SPVs at node } \textit{i.} \\ p_{i,j}^{\text{MDG_s}} & & \text{Available active, reactive grid power at node } \textit{i at time } \textit{t.} \\ p_{j}^{\text{MDG_s}} & & \text{Size (MW) of } \textit{jth unit of MDGs.} \\ r_{i,j}^{\text{SES_ct}}, & & \text{Size (MW) of } \textit{jth unit of SESSs at node } \textit{i.} \\ r_{i,j}^{\text{MES_e}}, & & \text{Converter + battery, converter, battery resistance of } \textit{jth unit of MESSs.} \\ t_{j}^{\text{MDG}}, & & \text{Converter + battery, converter, battery resistance and reactance of line } \textit{ik.} \\ r_{j}^{\text{MES_bt}}, & & \text{Converter + battery, converter, battery resistance of } \textit{jth unit of MESSs.} \\ t_{j}^{\text{MDG}}, & & \text{Total number of available MDGs,} \\ & & \text{MESSs units.} \\ T_{\text{CONVESSS}}, & & \text{Total number of RCs allowed to repair a damaged line simultaneously.} \\ \end{array}$	$S_{i,j}$	
Parameters used to maintain the ratio of active and reactive power outputs of MDGs, SDGs, and SPVs. M A Big-M constant. N Number of nodes/super-nodes. N_i^{SDG} , N_i^{SES} , Number of PDA-DERs (SDGs, SESSs, SPVs) at node i . Hourly solar irradiation profile. $p_{i,j}^{SDG_c}$, Active, reactive power capacity of j th unit of SDGs at node i . $p_{i,j}^{G}$, Active power capacity of j th unit of SPVs at node i . Active power capacity of j th unit of SPVs at node i . Available active, reactive grid power at node i at time t . Size (MW) of j th unit of MDGs. r_{ik} , x_{ik} , $r_{i,j}^{SES_bt}$, $r_{i,j}^{SES_bt}$, $r_{i,j}^{SES_bt}$, $r_{i,j}^{MES_bt}$, Converter $+$ battery, converter, battery resistance of j th unit of MESSs. t^{MDG} , t^{MES} Converter $+$ battery, converter, battery resistance of j th unit of MESSs. Total number of available MDGs, MESSs units. Total number of RCs allowed to repair a damaged line simultaneously.	EMES s	SESSS at flode t.
Parameters used to maintain the ratio of active and reactive power outputs of MDGs, SDGs, and SPVs. M A Big-M constant. N Number of nodes/super-nodes. N_i^{SDG} , N_i^{SES} , Number of PDA-DERs (SDGs, SESSs, SPVs) at node i . Hourly solar irradiation profile. $p_{i,j}^{SDG_c}$, Active, reactive power capacity of j th unit of SDGs at node i . $p_{i,j}^{G}$, Active power capacity of j th unit of SPVs at node i . Active power capacity of j th unit of SPVs at node i . Available active, reactive grid power at node i at time t . Size (MW) of j th unit of MDGs. r_{ik} , x_{ik} , $r_{i,j}^{SES_bt}$, $r_{i,j}^{SES_bt}$, $r_{i,j}^{SES_bt}$, $r_{i,j}^{MES_bt}$, Converter $+$ battery, converter, battery resistance of j th unit of MESSs. t^{MDG} , t^{MES} Converter $+$ battery, converter, battery resistance of j th unit of MESSs. Total number of available MDGs, MESSs units. Total number of RCs allowed to repair a damaged line simultaneously.	E_{j} ,	
Parameters used to maintain the ratio of active and reactive power outputs of MDGs, SDGs, and SPVs. M A Big-M constant. N Number of nodes/super-nodes. N_i^{SDG} , N_i^{SES} , Number of PDA-DERs (SDGs, SESSs, SPVs) at node i . Hourly solar irradiation profile. $p_{i,j}^{SDG_c}$, Active, reactive power capacity of j th unit of SDGs at node i . $p_{i,j}^{G}$, Active power capacity of j th unit of SPVs at node i . Active power capacity of j th unit of SPVs at node i . Available active, reactive grid power at node i at time t . Size (MW) of j th unit of MDGs. r_{ik} , x_{ik} , $r_{i,j}^{SES_bt}$, $r_{i,j}^{SES_bt}$, $r_{i,j}^{SES_bt}$, $r_{i,j}^{MES_bt}$, Converter $+$ battery, converter, battery resistance of j th unit of MESSs. t^{MDG} , t^{MES} Converter $+$ battery, converter, battery resistance of j th unit of MESSs. Total number of available MDGs, MESSs units. Total number of RCs allowed to repair a damaged line simultaneously.	$S_j^{\text{NILS}_S}$	
$\begin{array}{cccccccccccccccccccccccccccccccccccc$	k_1, k_2	Parameters used to maintain the ratio
$\begin{array}{lll} M & \text{A Big-M constant.} \\ N & \text{Number of nodes/super-nodes.} \\ N_i^{\text{SDG}}, N_i^{\text{SES}}, \\ N_i^{\text{SPV}} & \text{Number of PDA-DERs (SDGs, SESSs, SPVs) at node } i. \\ p_i^{\text{profile}} & \text{Hourly solar irradiation profile.} \\ p_{i,j}^{\text{SDG_c}}, \\ q_{i,j}^{\text{SDG_c}} & \text{Active, reactive power capacity of } j\text{th unit of SDGs at node } i. \\ p_{i,j}^{\text{SPV_c}} & \text{Active power capacity of } j\text{th unit of SPVs at node } i. \\ p_{i,t}^{\text{G}}, q_{i,t}^{\text{G}} & \text{Available active, reactive grid power at node } i \text{ at time } t. \\ p_i^{\text{MDG_s}} & \text{Size (MW) of } j\text{th unit of MDGs.} \\ r_{i,j}^{\text{SES_e}}, r_{i,j}^{\text{SES_ct}}, r_{i,j}^{\text{SES_ct}}, r_{i,j}^{\text{SES_ct}}, r_{i,j}^{\text{MES_e}}, r_{j}^{\text{MES_ct}}, r_{j}^{\text{MES_ct}}, r_{j}^{\text{MES_ct}}, r_{j}^{\text{MES}} & \text{Converter + battery, converter, battery resistance of } j\text{th unit of MESSs.} \\ t^{\text{MDG}}, t^{\text{MES}} & \text{Total number of available MDGs,} \\ MESSs units. \\ T^{\text{RC}} & \text{Total number of RCs allowed to repair a damaged line simultaneously.} \\ \end{array}$		of active and reactive power outputs of
$\begin{array}{lll} N & \text{Number of nodes/super-nodes.} \\ N_i^{\text{SDG}}, N_i^{\text{SES}}, & & \\ N_i^{\text{SPV}} & \text{Number of PDA-DERs (SDGs, SESSs, SPVs) at node } i. \\ P_i^{\text{profile}} & \text{Hourly solar irradiation profile.} \\ P_{i,j}^{\text{SDG_c}}, & & \\ Q_{i,j}^{\text{SDG_c}} & \text{Active, reactive power capacity of } j \text{th unit of SDGs at node } i. \\ P_{i,j}^{\text{SPV_c}} & \text{Active power capacity of } j \text{th unit of SPVs at node } i. \\ P_{i,j}^{\text{G}}, & & \text{Available active, reactive grid power at node } i \text{ at time } t. \\ P_{i,j}^{\text{MDG_s}} & & \text{Size (MW) of } j \text{th unit of MDGs.} \\ P_{i,j}^{\text{SES_e}}, & & \text{rij} & & \text{Converter + battery, converter, battery resistance of } j \text{th unit of SESSs at node } i. \\ P_{i,j}^{\text{MES_bt}} & & \text{Converter + battery, converter, battery resistance and reactance of line } i k. \\ P_{i,j}^{\text{MES_bt}} & & \text{Converter + battery, converter, battery resistance of } j \text{th unit of MESSs.} \\ P_{i,j}^{\text{MES_bt}} & & \text{Converter + battery, converter, battery resistance of } j \text{th unit of MESSs.} \\ P_{i,j}^{\text{MES_bt}} & & \text{Converter + battery, converter, battery resistance of } j \text{th unit of MESSs.} \\ P_{i,j}^{\text{MES_bt}} & & \text{Converter + battery, converter, battery resistance of } j \text{th unit of MESSs.} \\ P_{i,j}^{\text{MES_bt}} & & \text{Converter + battery, converter, battery resistance of } j \text{th unit of MESSs.} \\ P_{i,j}^{\text{MES_bt}} & & \text{Converter + battery, converter, battery resistance of } j \text{th unit of MESSs.} \\ P_{i,j}^{\text{MES_bt}} & & \text{Converter + battery, converter, battery resistance of } j \text{th unit of MESSs.} \\ P_{i,j}^{\text{MES_bt}} & & \text{Converter + battery, converter, battery resistance of } j \text{th unit of MESSs.} \\ P_{i,j}^{\text{MES_bt}} & & \text{Converter + battery, converter, battery resistance of } j \text{th unit of MESSs.} \\ P_{i,j}^{\text{MES_bt}} & & \text{Converter + battery, converter, battery resistance of } j \text{th unit of MESSs.} \\ P_{i,j}^{\text{MES_bt}} & & \text{Converter + battery, converter, battery resistance of } j \text{th unit of MESSs.} \\ P_{i,j}^{\text{MES_bt}} & & Converter + battery, converter, batt$		MDGs, SDGs, and SPVs.
$\begin{array}{lll} N_i^{\rm SDG}, N_i^{\rm SES}, \\ N_i^{\rm SPV} & {\rm Number \ of \ PDA-DERs \ (SDGs, \ SESSs, \ SPVs) \ at \ node \ i.} \\ p_t^{\rm profile} & {\rm Hourly \ solar \ irradiation \ profile.} \\ p_{i,j}^{\rm SDG_c}, \\ q_{i,j}^{\rm SDV_c} & {\rm Active, \ reactive \ power \ capacity \ of \ jth \ unit \ of \ SDGs \ at \ node \ i.} \\ p_{i,j}^{\rm SPV_c} & {\rm Active \ power \ capacity \ of \ jth \ unit \ of \ SPVs \ at \ node \ i.} \\ p_{i,j}^{\rm G}, q_{i,t}^{\rm G} & {\rm Available \ active, \ reactive \ grid \ power \ at \ node \ i \ at \ time \ t.} \\ p_{i,j}^{\rm MDG_s} & {\rm Size \ (MW) \ of \ jth \ unit \ of \ MDGs.} \\ r_{i,j}^{\rm SES_et}, r_{i,j}^{\rm SES_ct}, \\ r_{i,j}^{\rm SES_bt} & {\rm Converter \ + \ battery, \ converter, \ battery \ resistance \ of \ jth \ unit \ of \ MESSs \ at \ node \ i.} \\ r_{i,j}^{\rm MES_et}, r_{i,j}^{\rm MES_ct}, r_{i,$	M	A Big-M constant.
$\begin{array}{cccccccccccccccccccccccccccccccccccc$		Number of nodes/super-nodes.
$\begin{array}{cccccccccccccccccccccccccccccccccccc$	$N_i^{\text{SDG}}, N_i^{\text{SES}},$	
$\begin{array}{cccccccccccccccccccccccccccccccccccc$	N_i^{SPV}	Number of PDA-DERs (SDGs, SESSs,
$\begin{array}{cccccccccccccccccccccccccccccccccccc$		
$\begin{array}{cccccccccccccccccccccccccccccccccccc$	p_t^{profile}	Hourly solar irradiation profile.
unit of SDGs at node i . $p_{i,j}^{SPV_c}$ Active power capacity of j th unit of SPVs at node i . $p_{i,t}^{G}$, $q_{i,t}^{G}$ Available active, reactive grid power at node i at time t . $p_{j}^{MDG_s}$ Size (MW) of j th unit of MDGs. $r_{i,j}^{SES_et}$ Converter $+$ battery, converter, battery resistance of j th unit of SESSs at node i . r_{ik} , x_{ik} Resistance and reactance of line ik . $r_{j}^{MES_et}$ Converter $+$ battery, converter, battery resistance of j th unit of MESSs. t^{MDG} , t^{MES} Total number of available MDGs, MESSs units. T^{RC} Total number of RCs allowed to repair a damaged line simultaneously.	$n_{\text{out}}^{\text{SDG_c}}$	ı
unit of SDGs at node i . $p_{i,j}^{SPV_c}$ Active power capacity of j th unit of SPVs at node i . $p_{i,t}^{G}$, $q_{i,t}^{G}$ Available active, reactive grid power at node i at time t . $p_{j}^{MDG_s}$ Size (MW) of j th unit of MDGs. $r_{i,j}^{SES_et}$ Converter $+$ battery, converter, battery resistance of j th unit of SESSs at node i . r_{ik} , x_{ik} Resistance and reactance of line ik . $r_{j}^{MES_et}$ Converter $+$ battery, converter, battery resistance of j th unit of MESSs. t^{MDG} , t^{MES} Total number of available MDGs, MESSs units. T^{RC} Total number of RCs allowed to repair a damaged line simultaneously.	SDG_c,	Active reactive power conseity of ith
$\begin{array}{lll} p_{i,j}^{\mathrm{SPV_c}} & \text{Active power capacity of } j \text{th unit of SPVs at node } i. \\ p_{i,t}^{\mathrm{G}}, q_{i,t}^{\mathrm{G}} & \text{Available active, reactive grid power at node } i \text{ at time } t. \\ p_{j}^{\mathrm{MDG_s}} & \text{Size (MW) of } j \text{th unit of MDGs.} \\ r_{i,j}^{\mathrm{SES_e}}, r_{i,j}^{\mathrm{SES_ct}}, & \\ r_{i,j}^{\mathrm{SES_bt}} & \text{Converter} + \text{battery, converter, battery resistance of } j \text{th unit of SESSs at node } i. \\ r_{ik}, x_{ik} & \text{Resistance and reactance of line } i k. \\ r_{j}^{\mathrm{MES_et}}, r_{j}^{\mathrm{MES_ct}}, & \\ r_{j}^{\mathrm{MES_bt}} & \text{Converter} + \text{battery, converter, battery resistance of } j \text{th unit of MESSs.} \\ t^{\mathrm{MDG}}, t^{\mathrm{MES}} & \text{Total number of available MDGs, MESSs units.} \\ T^{\mathrm{RC}} & \text{Total number of RCs allowed to repair a damaged line simultaneously.} \\ \end{array}$	$q_{i,j}$	
SPVs at node i . $p_{i,t}^{G}, q_{i,t}^{G}$ Available active, reactive grid power at node i at time t . $p_{j}^{MDG_s}$ Size (MW) of j th unit of MDGs. Size (MW) of j th unit of MDGs. Converter j battery resistance of j th unit of SESSs at node j . Resistance and reactance of line j th. j th	SPV c	
$\begin{array}{ll} p_{i,t}^{\rm G}, q_{i,t}^{\rm G} & {\rm Available\ active,\ reactive\ grid\ power\ at} \\ p_{j}^{\rm MDG_s} & {\rm Size\ (MW)\ of\ } j {\rm th\ unit\ of\ MDGs.} \\ \\ r_{i,j}^{\rm SES_e}, r_{i,j}^{\rm SES_ct}, \\ r_{i,j}^{\rm SES_bt} & {\rm Converter\ } + {\rm battery,\ converter,\ battery} \\ resistance\ of\ j {\rm th\ unit\ of\ SESSs\ at\ node\ } i. \\ \\ r_{jk}^{\rm MES_e}, r_{j}^{\rm MES_ct}, \\ r_{j}^{\rm MES_bt} & {\rm Converter\ } + {\rm battery,\ converter,\ battery} \\ resistance\ of\ j {\rm th\ unit\ of\ MESSs.} \\ \\ t^{\rm MDG}, t^{\rm MES} & {\rm Total\ number\ of\ available\ MDGs,\ MESSs\ units.} \\ \\ T^{\rm RC} & {\rm Total\ number\ of\ RCs\ allowed\ to\ repair\ a\ damaged\ line\ simultaneously.} \end{array}$	$p_{i,j}^{si}$	
node i at time t . $p_{j}^{\text{MDG_s}}$ Size (MW) of j th unit of MDGs. $r_{i,j}^{\text{SES_e}}$, $r_{i,j}^{\text{SES_ct}}$, $r_{i,j}^{\text{SES_bt}}$ Converter $+$ battery, converter, battery resistance of j th unit of SESSs at node i . r_{ik} , x_{ik} Resistance and reactance of line ik . $r_{j}^{\text{MES_et}}$, $r_{j}^{\text{MES_ct}}$, $r_{j}^{\text{MES_bt}}$ Converter $+$ battery, converter, battery resistance of j th unit of MESSs. t^{MDG} , t^{MES} Total number of available MDGs, MESSs units. T^{RC} Total number of RCs allowed to repair a damaged line simultaneously.	C C	
$\begin{array}{ll} p_{j}^{\text{MDG_s}} & \text{Size (MW) of } j \text{th unit of MDGs.} \\ r_{i,j}^{\text{SES_e}}, r_{i,j}^{\text{SES_ct}}, \\ r_{i,j}^{\text{SES_bt}} & \text{Converter + battery, converter, battery} \\ resistance of } j \text{th unit of SESSs at node } i. \\ r_{ik}, x_{ik} & \text{Resistance and reactance of line } ik. \\ r_{j}^{\text{MES_e}}, r_{j}^{\text{MES_ct}}, \\ r_{j}^{\text{MES_bt}} & \text{Converter + battery, converter, battery} \\ resistance of } j \text{th unit of MESSs.} \\ t^{\text{MDG}}, t^{\text{MES}} & \text{Total number of available MDGs,} \\ MESSs units.} \\ T^{\text{RC}} & \text{Total number of RCs allowed to repair a damaged line simultaneously.} \end{array}$	$p_{i,t}^{\mathrm{G}}, q_{i,t}^{\mathrm{G}}$	
$r_{i,j}^{\text{SES}}$, $r_{i,j}^{\text{SES}}$, $r_{i,j}^{\text{SES}}$, $r_{i,j}^{\text{SES}}$ Converter + battery, converter, battery resistance of j th unit of SESSs at node i . r_{ik} , x_{ik} Resistance and reactance of line ik . r_{j}^{MES} , r_{j}^{MES} , r_{j}^{MES} Converter + battery, converter, battery resistance of j th unit of MESSs. t^{MDG} , t^{MES} Total number of available MDGs, MESSs units. T^{RC} Total number of RCs allowed to repair a damaged line simultaneously.	MDC	
$r_{i,j}^{\text{SES}}$, $r_{i,j}^{\text{SES}}$, $r_{i,j}^{\text{SES}}$, $r_{i,j}^{\text{SES}}$ Converter + battery, converter, battery resistance of j th unit of SESSs at node i . r_{ik} , x_{ik} Resistance and reactance of line ik . r_{j}^{MES} , r_{j}^{MES} , r_{j}^{MES} Converter + battery, converter, battery resistance of j th unit of MESSs. t^{MDG} , t^{MES} Total number of available MDGs, MESSs units. T^{RC} Total number of RCs allowed to repair a damaged line simultaneously.	$p_i^{\text{MDG_s}}$	Size (MW) of <i>j</i> th unit of MDGs.
resistance of j th unit of SESSs at node i . Resistance and reactance of line ik . Resistance and reactance of line ik . Converter $+$ battery, converter, battery resistance of j th unit of MESSs. t^{MDG} , t^{MES} Total number of available MDGs, MESSs units. T^{RC} Total number of RCs allowed to repair a damaged line simultaneously.	$r_{i,i}^{SES_e}, r_{i,i}^{SES_ct},$	
resistance of j th unit of SESSs at node i . Resistance and reactance of line ik . Resistance and reactance of line ik . Converter $+$ battery, converter, battery resistance of j th unit of MESSs. t^{MDG} , t^{MES} Total number of available MDGs, MESSs units. T^{RC} Total number of RCs allowed to repair a damaged line simultaneously.	rSES_bt	Converter + battery converter battery
r_{ik}, x_{ik} Resistance and reactance of line ik . $r_{j}^{\text{MES}_e}, r_{j}^{\text{MES}_ct},$ $r_{j}^{\text{MES}_bt}$ Converter + battery, converter, battery resistance of j th unit of MESSs. $t^{\text{MDG}}, t^{\text{MES}}$ Total number of available MDGs, MESSs units. T^{RC} Total number of RCs allowed to repair a damaged line simultaneously.	' i,j	-
$\begin{array}{cccccccccccccccccccccccccccccccccccc$	r., r.,	
$r_j^{MES_bt}$ Converter + battery, converter, battery resistance of j th unit of MESSs. t^{MDG} , t^{MES} Total number of available MDGs, MESSs units. T^{RC} Total number of RCs allowed to repair a damaged line simultaneously.	MES_e MES_ct	Resistance and reactance of fine ix.
resistance of j th unit of MESSs. t^{MDG} , t^{MES} Total number of available MDGs, MESSs units. T^{RC} Total number of RCs allowed to repair a damaged line simultaneously.	r_j , r_j ,	~ .
$t^{\mathrm{MDG}}, t^{\mathrm{MES}}$ Total number of available MDGs, MESSs units. T^{RC} Total number of RCs allowed to repair a damaged line simultaneously.	$r_j^{mLS_oi}$	
$T^{\rm RC}$ MESSs units. Total number of RCs allowed to repair a damaged line simultaneously.	MDC MES	
TRC Total number of RCs allowed to repair a damaged line simultaneously.	$t^{\text{MIDG}}, t^{\text{MES}}$	
damaged line simultaneously.	D.C.	
· · · · · · · · · · · · · · · · · · ·	$T^{\kappa C}$	
Binary		damaged line simultaneously.
4 7 7	Binary	

variables

 $\chi_{i,j,t}^{\text{MDG}}, \chi_{i,j,t}^{\text{MESS}}$

Binary variable to denote repair activity $\alpha_{ik,m,t}$ of RC m with respect to line ik at time t. Binary variable to denote jth unit of MERs (MDGs, MESSs) in reference to node i at time t.

Auxiliary binary variable. $S_{ik,m,t}$ $u_{ik,t}$

Binary variable to denote operating status of line ik at time t.

Continuous variables

$\ell_{ik,t}$	Squared of current flow on line ik at time
$p_{i,j,t}^{\mathrm{MES_l}}$	t.Power loss in jth unit of MESSs at nodei at time t.
$p_{i,j,t}^{\mathrm{SES_l}}$	Power loss in <i>j</i> th unit of SESSs at node <i>i</i> at time <i>t</i> .
$p_{i,j,t}^{g}, q_{i,j,t}^{g}, \\ g \in \Omega_{ders}$	Active, reactive power output of <i>j</i> th unit of DERs at node <i>i</i> at time <i>t</i> .
	or B Bris at nous : at time !:

 $p_{i,j,t}^{\mathrm{g}}, q_{i,j,t}^{\mathrm{g}},$ Active, reactive power output of jth unit of MERs at node i at time t. $p_{i,t}^{\mathrm{L}}, q_{i,t}^{\mathrm{L}}$ Active, reactive power supplied to node i at time t.

Active, reactive power flow of line ik at $p_{ik,t}, q_{ik,t}$ time t. Squared of voltage at node i at time t. $v_{i,t}$

I. INTRODUCTION

In recent years, high-impact low-frequency (HILF) events such as hurricanes, ice storms, earthquakes, cyber-attacks, et cetera, are happening at a higher frequency [1]. Impacts of such HILF events are colossal [2], and it has been reported that such events may cause loss of billions of dollars to the United States every year [3]. An important measure to mitigate this issue is improving the resilience of critical infrastructure (CI) systems such as electricity, water delivery, transportation, communication systems, health, finance, et cetera. The power system plays a fundamental role since all other CI systems rely heavily on electricity. Unfortunately, there is no commonly accepted definition for the resilience of power systems thus far. According to [4], power system resilience can be defined as "the ability to prepare for and adapt to changing conditions and withstand and recover rapidly from extreme outages." Therefore, strategies for fast and effective restoration of power supply after extreme events play an essential role in power system resilience.

A. LITERATURE REVIEW

The early-stage research activities adopted a top-down strategy for power system restoration, i.e., the restoration of bulk transmission systems is followed by the restoration of distribution networks. However, with the proliferation of distributed energy resources (DERs) in the last two decades [5], distribution networks possess a significant amount of energy resources, which can be utilized to start the restoration locally to facilitate the effective restoration of overall power systems. Note that the term DERs collectively refers to all types of distributed energy resources in this paper. Examples are static (or location-fixed) diesel generators (SDGs), static energy storage systems (SESSs), and static photovoltaic systems (SPVs). The term static is adopted



to differentiate DERs, whose locations are fixed, from mobile resources. The utilization of post-disaster available distributed energy resources (PDA-DERs) with the formation of self-sufficient microgrids in distribution network restoration has been extensively studied in the last fifteen years [6]. Note that PDA-DERs refer to the DERs that survive a disaster. In [6], a sequence of control actions in black-start restoration using low-voltage microgrids is described in detail. Literature [7] describes the minimum spanning tree search method to maximize load restoration by minimizing switching operation in microgrids-embedded distribution networks [8]. A multi-stage restoration method is proposed in [9] to maximize restoration of out-of-service loads using distributed generators [10].

Furthermore, in [11], the formation of microgrids with the three-phase operation of PDA-DERs is considered to expedite the restoration process. The dynamically changing boundary of microgrids is considered for load restoration in [12]. Multi-time step service restoration under cold load pickup conditions considering inter-temporal constraints of PDA-DERs is investigated in [13]. The utilization of PDA-DERs for service restoration to critical loads in secondary networks is studied in [14]. Technical issues associated are also analyzed. In [15], critical load restoration with available PDA-DERs considering post-restoration failures is studied. In [16], variable and fixed time-step restoration models are proposed to achieve optimal restoration performance under the presence of remotely controllable and manually operated switches and dispatchable PDA-DERs. A multi-microgrids framework for the black-start of distribution networks is proposed in [17] to facilitate the integration of PDA-DERs. A distributed multi-agent coordination scheme is developed in [18] to improve the coordination of multiple microgrids in distribution network restoration. In summary, the literature illustrates that the formation of disaster-induced islands (or microgrids) with PDA-DERs to restore electric service in distribution networks immediately after a severe disaster is an effective strategy.

Recently, some researchers started exploring the possibility of using emergency response resources (ERRs), such as repair crews (RCs) and mobile energy resources (MERs) [19], to accelerate the power distribution systems restoration after a disaster. In this paper, the term MERs collectively represents all types of truck-mounted mobile power/energy sources. Different types of MERs include mobile diesel generators (MDGs) and mobile energy storage systems (MESSs) [20]. Capacities of MDGs and MESSs are generally described by kW and kVar, kWh and kVA, respectively. In [21], scenario-based pre-positioning and real-time allocation of MDGs are proposed. The utilization of MESSs in enhancing distribution system resilience is studied in [22]. Adaptive multi-microgrid formation leveraging MDGs is investigated in [23]. Reference [24] describes the scenario-based routing and scheduling of MDGs and MESSs to increase the survivability of electric service to critical loads during and after a HILF event. The logistics of routing MERs and RCs to supply critical loads is studied in [25]. Scenario-based allocation of MDGs considering three stages of a disaster (planning stage, preventive stage, and emergency response stage) is proposed in [26]. Authors in [27] proposed a framework considering network reconfiguration and pre-located MDGs to reduce the impact of disasters. A two-step optimization strategy that integrates a pre-disaster preparedness plan and a post-disaster resource re-allocation procedure to optimize the resilience of the power distribution network against hurricanes is proposed in [28].

In [29], various strategies for enhancing distribution system resilience are synthesized by integrating mobile energy storage systems, microgrid resources, and network reconfiguration to maintain system functionality during major power disruptions. A new mobility model for MERs is proposed for efficient routing, ensuring rapid service restoration and resilience against unexpected events in [30]. Strategies for improving isolated distribution system survivability through coordinated mobile energy storage and demand response, optimizing fuel consumption and demand under extreme scenarios, are also presented in [31]. Additionally, a twostage restoration approach to reduce load outages in the face of seismic events using mobile power sources is evaluated in [32]. A two-step model for the optimal allocation of stationary and mobile energy storage systems is introduced, enhancing reliability in high renewable energy penetration environments in [33].

Moreover, a multiagent reinforcement learning-based framework is proposed considering communication disruptions in microgrids during extreme events in [34]. The introduction of separable MESSs, combined with emergency generators and fuel tankers, has demonstrated improved resilience in distribution systems in [35]. A decision-making framework for MESSs is developed to manage battery delivery and relocation during grid outages, with strategies tailored for different outage phases in [36]. For post-disaster scenarios in pelagic island energy systems, a self-sustaining strategy employing mobile multi-energy storages is proposed, integrating them with diesel generators and desalination devices in [37]. An integrated optimization model for unbalanced distribution system restoration post-major outages has coordinated distributed energy resources and repair crews, proving its effectiveness in [38]. Another study has introduced a restoration mechanism for power distribution systems using mobile energy storage systems and stochastic renewable energy sources, reformulated into a mixed-integer linear programming model, enhancing system resilience against high-impact, low-probability incidents in [39]. Lastly, a robust optimization method for enhancing resilience during ice storms is presented, focusing on the optimal routing of mobile de-icing devices on congested roads and integrating de-icing schedules with power system operations in [40]. Existing research shows that coordination of MERs and RCs has a high potential for effective service restoration in distribution networks.



B. RESEARCH GAP AND CONTRIBUTIONS

Even though the restoration of power distribution systems has been extensively studied [41] in recent years, there are still some challenges in solving the large-scale postdisaster restoration model [21], [22], [23], [24], [25]. The main challenges arise from 1) the nonlinearity of the power flow, PDA-DERs, and MERs models, 2) the huge number of decision variables (both continuous and binary decision variables), and 3) the combinatorial nature of the post-disaster optimization model. Therefore, different types of solution methods are proposed to handle the computational complexity of the restoration models in the literature. Existing solution methods can be broadly categorized into two. In the first type of method, the original mixed-integer non-linear program (MINLP) restoration model is either linearized and reformulated as the mixed-integer linear program (MILP) model as in [19], [21], [23], [24], [25], [27], [29], [30], [31], [32], [33], [35], [38], and [39] (detailed literature review of these references is provided in Section I-A) or convexified and solved as a convex model as in [40]. Nonetheless, we have shown in Section III that the linear and convex models alone do not achieve the computational efficiency desired for a complex post-disaster model studied in this paper, especially for a problem that simultaneously optimizes the routing of RCs, and locating and scheduling of operation of MERs and PDA-DERs. Therefore, the second type of method decomposes the large-scale restoration model into multiple smaller problems, which are then solved in an iterative fashion until convergence by using algorithms such as scenario decomposition algorithm [21], progressive hedging algorithm [22], benders decomposition and columnand-constraint generation algorithms [40], etc. However, the iterative algorithms have their own limitations, such as stability and scalability, and may not even converge while coordinating mixed-integer programs at times.

Therefore, this paper proposes a non-iterative computationally tractable restoration framework for solving the large-scale restoration model by leveraging super-node approximation (SNA) and convex hulls relaxation (CHR), as shown in Figure 1. The SNA reduces the size of the restoration model without significant loss of accuracy (refer to the discussion in Section II-C for more details), while the CHR, which is the tightest of all convex relaxations, convexifies the overall optimization model to reduce the computational burden further. To our knowledge, leveraging a combination of CHR and SNA to reduce the computational burden of the post-disaster restoration model is new. Compared to standalone linear and convex models, the proposed method is computationally very efficient (see Table 6 in Section III). In addition, it does not involve any iterative procedures, unlike decomposition-based methods. In summary, the key contributions of this paper can be summarized as follows:

 From the engineering perspective, emergency response resources (ERRs) like MERs and RCs are co-optimized with PDA-DERs to minimize the impact of disasters on customers.

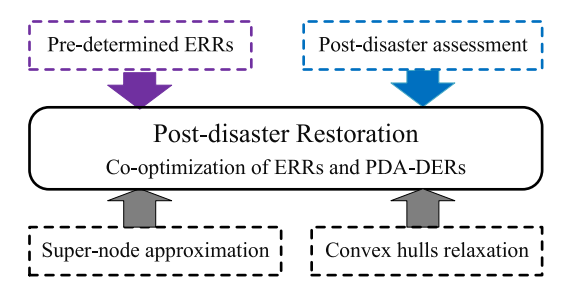


FIGURE 1. The proposed framework for distribution system restoration.

2) From the mathematical perspective, the combination of super-node approximation (SNA) and convex hulls relaxation (CHR) is introduced to reduce the computational burden of the combinatorial and non-convex non-linear nature of the post-disaster restoration model. SNA reduces the problem size (combinatorial nature) without significant loss of accuracy (refer to the discussion in Section II-C for more details). Furthermore, the CHR convexifies the overall optimization model (nonconvex, non-linear nature) to reduce the computational burden further.

In Figure 1, the PDA-DERs are referred to as the grid-connected DERs that survive the disaster. As such, the pre-determined ERRs (such as MERs and RCs) and PDA-DERs are co-optimized to minimize the impact of a disaster on customers. Nonetheless, the ERRs must be allocated and pre-positioned a few days before the disaster. Scenario-based methods for pre-allocating MERs are investigated in [22], [26], and [28]. This paper is focused on post-disaster restoration; therefore, for the pre-disaster planning (and ERRs allocation) and long-term recovery of the system after a disaster, readers are referred to [22], [26], and [28] and references therein. The rest of the paper is organized as follows: Section II describes the post-disaster restoration model along with CHR and SNA. Section III provides case studies and results, and Section IV concludes with the conclusion and the potential future research.

II. POST-DISASTER RESTORATION

Different types of ERRs (MERs and RCs) are prepared by the power utility before a disaster. After the disaster, the distribution system operator (DSO) performs post-disaster damage assessment and routes and dispatches MERs and RCs to restore electric service as quickly as possible. The post-disaster restoration model is built to help DSOs restore electric service quickly and repair severely damaged distribution lines. This section presents an optimization model to co-optimize routing and dispatch of pre-allocated 1) MERs in coordination with PDA-DERs to supply the outage loads and 2) repair crews (RCs) to repair damaged lines. Due to inherent nonlinearity and the combinatorial nature of the problem, the original optimization model is computationally intractable. For rapidly obtaining an accurate solution to this complex optimization problem, two techniques, i.e.,



convex-hull relaxation and super-node approximation, are introduced, which significantly improve the computational efficiency.

A. PROBLEM FORMULATION

In the restoration process, all available ERRs (including MERs and repair crews) and PDA-DERs should be optimally coordinated based on the network damage information obtained from the post-disaster damage assessment. Choosing an objective function of minimizing the unserved energy, the post-disaster restoration model is given as follows:

Min.
$$\sum_{i} \sum_{t} \left(\overline{p}_{i,t}^{L} - p_{i,t}^{L} \right) \Delta t$$
 (1a)

$$p_{i,t}^{L} \le p_{i,t}^{L} \le \overline{p}_{i,t}^{L} \tag{1b}$$

$$q_{i,t}^{L} \le q_{i,t}^{L} \le \overline{q}_{i,t}^{L} \tag{1c}$$

$$-(1-u_{ik,t})M \le v_{i,t}-v_{k,t}-2(r_{ik}p_{ik,t}+x_{ik}q_{ik,t})$$

$$+\left((r_{ik})^2 + (x_{ik})^2\right)\ell_{ik,t} \le \left(1 - u_{ik,t}\right)M$$
 (1d)

$$(p_{ik,t})^2 + (q_{ik,t})^2 = v_{i,t}\ell_{ik,t}$$
 (1e)

$$\underline{v}_i \le v_{i,t} \le \overline{v}_i \tag{1f}$$

$$0 \le \ell_{ik,t} \le \overline{\ell}_{ik} \tag{1g}$$

$$\left(p_{ik,t}\right)^2 + \left(q_{ik,t}\right)^2 \le \left(\overline{S}_{ik}\right)^2 \tag{1h}$$

$$0 \le p_{i,i,t}^{\text{MDG}} \le \chi_{i,i,t}^{\text{MDG}} p_{i}^{\text{MDG_s}}, \forall i, \forall j, \forall t$$
 (1i)

$$(p_{ik,t})^{2} + (q_{ik,t})^{2} \leq (\overline{S}_{ik})^{2}$$

$$(1h)$$

$$0 \leq p_{i,j,t}^{MDG} \leq \chi_{i,j,t}^{MDG} p_{j}^{MDG_s}, \forall i, \forall j, \forall t$$

$$0 \leq p_{i,j,t}^{SDG} \leq p_{i,j}^{SDG_c}$$

$$(1j)$$

$$k_1 * p_{i,j,t}^{g} \le q_{i,j,t}^{g} \le k_2 * p_{i,j,t}^{g}, \forall g \in \Omega_{res}$$
 (1k)

$$K_1 * P_{i,j,t} \le q_{i,j,t} \le K_2 * P_{i,j,t}, \forall g \in \Sigma^{2} res$$

$$N \qquad t \qquad \qquad ($$

$$0 \le E_j^{\text{ES_spl}} - \sum_{i=1}^{N} \sum_{\tau=1}^{t} \left(p_{i,j,\tau}^{\text{ES}} + p_{i,j,\tau}^{\text{ES_l}} \right) \Delta t$$

$$\leq E_{j}^{\mathrm{ES_s}}, \forall i, \forall j, \forall t,$$
 (11)

$$\left(p_{i,j,t}^{\text{MES}}\right)^2 + \left(q_{i,j,t}^{\text{MES}}\right)^2 \le \chi_{i,j,t}^{\text{MES}} \left(S_j^{\text{MES_s}}\right)^2$$
 (1m)

$$\left(p_{i,j,t}^{\text{SES}}\right)^2 + \left(q_{i,j,t}^{\text{SES}}\right)^2 \le \left(S_{i,j}^{\text{SES_c}}\right)^2 \tag{1n}$$

$$r_j^{\text{ES_e}} \left(p_{i,j,t}^{\text{ES}} \right)^2 + r_j^{\text{ES_ct}} \left(q_{i,j,t}^{\text{ES}} \right)^2 = p_{i,j,t}^{\text{ES_l}} v_{i,t}$$
 (10)

$$p_{i,t}^{G} + \sum_{j=1}^{l^{\text{MDG}}} p_{i,j,t}^{\text{MDG}} + \sum_{j=1}^{l^{\text{MES}}} p_{i,j,t}^{\text{MES}}$$

$$+ \sum_{j=1}^{N_{i}^{\text{SDG}}} p_{i,j,t}^{\text{SDG}} + \sum_{j=1}^{N_{i}^{\text{SES}}} p_{i,j,t}^{\text{SES}} + \sum_{j=1}^{N_{i}^{\text{SPV}}} p_{i,j,t}^{\text{SPV}} - p_{i,t}^{\text{L}} = \sum_{j} \left(p_{ji,t} - r_{ji} \ell_{ji,t} \right) + \sum_{k} p_{ik,t}$$
 (1p)

$$q_{i,t}^{\text{G}} + \sum_{i=1}^{t^{\text{MDG}}} q_{i,j,t}^{\text{MDG}} + \sum_{j=1}^{t^{\text{MES}}} q_{i,j,t}^{\text{MES}}$$

$$+ \sum_{j=1}^{N_{i}^{SDG}} q_{i,j,t}^{SDG} + \sum_{j=1}^{N_{i}^{SES}} q_{i,j,t}^{SES} + \sum_{j=1}^{N_{i}^{SPV}} q_{i,j,t}^{SPV} - q_{i,t}^{L} = \sum_{i} (q_{ji,t} - x_{ji}\ell_{ji,t}) + \sum_{k} q_{ik,t}$$
(1q)

$$\sum_{i} \chi_{i,j,t}^{g} \le 1, \forall g \in \Omega_{mers}, \forall j, \forall t$$
 (1r)

 $\chi_{i,i,t+\tau}^{g} + \chi_{n,i,t}^{g} \leq 1, g \in \Omega_{mers}, \forall j, \forall t, j \in \mathcal{G}_{mers}$

$$\forall \tau \in \{1, \dots, \mathsf{TT}_{i,n}\}\tag{1s}$$

 $\chi_{i,i,t}^{g} = \chi_{i,i,t-1}^{g}, g \in \Omega_{mers}, \forall i, \forall j,$

$$\forall t \in \{2, 3, \dots, T\} \text{ (optional)} \tag{1t}$$

$$-u_{ik,t}M \le p_{ik,t} \le u_{ik,t}M \tag{1u}$$

$$-u_{ik,t}M \le q_{ik,t} \le u_{ik,t}M \tag{1v}$$

$$u_{ik,t} \ge u_{ik,t-1} \tag{1w}$$

$$\sum_{ik} \alpha_{ik,m,t} \le 1, \forall m, \forall t \tag{1x}$$

$$\sum_{m} \alpha_{ik,m,t} \le T^{\text{RC}}, \forall ik, \forall t$$
 (1y)

 $\alpha_{ji,m,t+\tau} + \alpha_{ik,m,t} \leq 1, \forall m, \forall t,$

$$\tau \in \{1, \dots, \mathsf{TT}_{ji, ik}\}\tag{1z}$$

$$\alpha_{ik,m,t} \le \alpha_{ik,m,t-1} + s_{ik,m,t} \tag{1aa}$$

$$\sum s_{ik,m,t} \le 1 \tag{1ab}$$

$$u_{ik,t+1} \le \frac{\sum_{m} \sum_{\tau=1}^{t} \alpha_{ik,m,\tau}}{RT_{ik}}, \forall ik$$
 (1ac)

$$\sum_{ik} \sum_{t} \alpha_{ik,m,t} \le RC_m^{c}. \tag{1ad}$$

The MERs allocation variables $(\chi_{i,j,t}^{\text{MDG}}, \chi_{i,j,t}^{\text{MES}})$ and variables related to repair activity of RCs $(\alpha_{ik,m,t})$ and status of damaged lines $(u_{ik,t})$ are the decision variables in the post-disaster restoration model. Note that binary variable $\chi_{i,j,t}^{\text{MDG}} = 1$ implies that jth unit of MDG is at node i at time t while binary variable $u_{ik,t} = 1$ represents that line ik (line connecting nodes i and k) is operating at time t. Inequalities (1b) and (1c) are load limits. The DistFlow model [5], [42] is adopted to model power flows as in (1d) and (1e). The Big-M method is employed in (1d) to force the voltage relationship between nodes connected by operating lines only. Voltage limits are imposed by the constraint (1f). Thermal and power limits of lines are enforced by constraints (1g) and (1h), respectively.

Constraints (1i)-(1n) describe the operating constraints (including state of charge constraints) of MERs and PDA-DERs in the post-disaster restoration model. Note that MDGs, SDGs, MESSs, and SESSs are considered dispatchable, while SPVs are considered non-dispatchable in this paper. A high-fidelity second-order model [43] is adopted to model the battery energy storage systems. The power loss due to charging and discharging in MESSs and SESSs is modeled by constraints (10). The nodal power balance



is achieved via equations (1p) and (1q). Constraint (1r) ensures that an MER unit is connected to one node at a time. Constraint (1s) means that an MER takes $TT_{i,n}$ time period to travel from node i to node n. The proposed model without the optional constraint (1t) allows the travel of MERs in the network. However, constraint (1t) can be enforced to optimally fix the locations of MERs for the entire restoration window. This is particularly useful in a post-disaster system without grid power where routing MERs in the network may not be justified as MERs cannot supply the customers during the travel. Constraints (1u) and (1v) are used to prevent power flow on lines that are damaged and not repaired yet. At the start of the restoration window, the operating status of damaged lines is set to 0. Constraint (1w) maintains that once a line is repaired at time t, it remains operable for the rest of the restoration window.

Constraints (1x)-(1ad) describe the dispatch of repair crews (RCs). Binary variable $\alpha_{ik,m,t}$ provides repair activity of RC m in reference to line ik at time t. If $\alpha_{ik,m,t} = 1$, RC m is repairing line ik at time t. If $\alpha_{ik,m,t} = 0$, RC m is not repairing line ik at time t. Constraint (1x) represents that an RC can work at only one line at a time. Constraint (1y) indicates that there should not be more than T^{RC} RCs that are working on repairing one power line at the same time. Constraint (1z) means that RC m spends $TT_{ji,jk}$ time period to travel from line ji to line ik. For a distribution network with a small geographical area, travel time within the network is relatively short and negligible compared to repair times of damaged lines. In such a case, travel time parameter TT_{ii.ik} in constraint (1z) can be set to 0. Constraints (1aa) and (1ab) represent that the repair work of a line should be completed in consecutive steps. Note that $\alpha_{lk,m,t}$ is assumed to be zero at the beginning (i.e., at t = 0), meaning repair activity of RCs is not started at t = 0. Constraint (1ac) represents that RCs should spend a minimum of RTik time repairing a damaged line ik before the status of the damaged line ik can be changed to operating. Constraint (1ad) enforces capacity limits of RCs.

Note that this paper aims to obtain optimal locations of MERs and an optimal repair order and schedule for damaged lines to establish the skeleton of a severely damaged distribution system where there is no electric path between many nodes due to damage to lines. Therefore, radiality constraints are not included in the formulation as radiality constraints are used to re-configure distribution systems where multiple electric paths exist between nodes [44]. Lastly, we assume that the loads and distribution lines are not equipped with switches.

B. CONVEX HULLS RELAXATION

The post-disaster restoration model presented in Section II-A is a mixed-integer non-linear program (MINLP) problem. Non-convexity (non-linearity) comes from the power flow equation (1e) and energy storage model (1o). Such MINLP problems of larger test systems are computationally expensive. Moreover, the global optimality of the obtained solution cannot be guaranteed. Therefore, in the literature, the original MINLP restoration model is either linearized as a mixed-integer linear program (MILP) as in [19], [21], [23], [24], [25], [27], [29], [30], [31], [32], [33], [35], [38], and [39] or convexified as a mixed-integer second-order cone program (MISOCP) as in [40]. The linear models are obtained by ignoring the current term in the power flow and are less accurate, while the second-order cone program (SOCP) may not always produce the tightest convex relaxation [43]. Therefore, we have leveraged convex hulls relaxation [45], which is considered one of the tightest convex relaxation of the DistFlow model in radial networks, to convexify the original MINLP problem into a mixed-integer convex program (MICP) problem in this paper. It has been shown in [45] that a MICP problem is much more computationally tractable than a MINLP problem of the same size and tighter than the MISOCP form of the same problem.

Within the bounds of system constraints (1f)-(1h), convex hulls relaxation of non-linear non-convex power flow constraint (1e) is given by (2). Convex hulls relaxation of non-convex MESSs and SESSs constraint (10) is given by (3).

$$p_{ik,t}^2 + q_{ik,t}^2 \le v_{i,t} \ell_{ik,t} \tag{2a}$$

$$\overline{S}_{ik}^2 v_i + \underline{v}_i \overline{v}_i \ell_{ik} \le \overline{S}_{ik}^2 (\underline{v}_i + \overline{v}_i)$$
 (2b)

$$r_{j}^{\text{ES_e}} \left(p_{i,j,t}^{\text{ES_}} \right)^{2} + r_{j}^{\text{ES_ct}} \left(q_{i,j,t}^{\text{ES_}} \right)^{2} \le p_{i,j,t}^{\text{ES_l}} v_{i,t}$$
(3a)

$$r_{j}^{ES_bt} (q_{i,j,t}^{\text{ES_}})^{2} + p_{i,j,t}^{\text{ES_l}} \underline{v}_{i} \le (S_{j}^{ES_s})^{2} r_{j}^{\text{ES_e}}$$
(3b)

$$(S_{j}^{ES_s})^{2} v_{i,t} + \underline{v}_{i} \overline{v}_{i} p_{i,j,t}^{\text{ES_l}} \le (S_{j}^{ES_s})^{2} (\underline{v}_{i} + \overline{v}_{i})$$
(3c)

$$\sum_{i}^{ES_{-}bt} (q_{i,i,t}^{ES_{-}})^2 + p_{i,i,t}^{ES_{-}1} \underline{v}_i \le (S_i^{ES_{-}s})^2 r_i^{ES_{-}e}$$
 (3b)

$$(S_i^{ES_s})^2 v_{i,t} + \underline{v_i} \overline{v_i} p_{i,j,t}^{ES_1} \le (S_j^{ES_s})^2 (\underline{v_i} + \overline{v_i}) \quad (3c)$$

Replacing (1e) and (1o) with (2) and (3), respectively, the MINLP model is relaxed to a mixed-integer convex program (MICP), which is computationally more tractable. However, with the MICP formulation, the optimal restoration problem for a relatively large distribution system like the IEEE 123-node test feeder is still challenging to solve. To further mitigate this computational efficiency issue, the super-node approximation (SNA) is introduced in the following subsection.

C. SUPER-NODE APPROXIMATION FOR DIMENSION **REDUCTION**

1) OVERVIEW OF SNA

The super-node approximation is introduced herein to reduce the dimension of large-scale post-disaster systems, which, in turn, reduces the computational burden of the problem. A similar dimension reduction approximation referred to as the vertex collapse technique is used in graph theory [46], [47]. A disaster-impacted IEEE 13-node test feeder, shown in Figure 2, is used to illustrate the super-node approximation in the context of distribution system restoration. After the disasters, the feeder is divided into four islands due



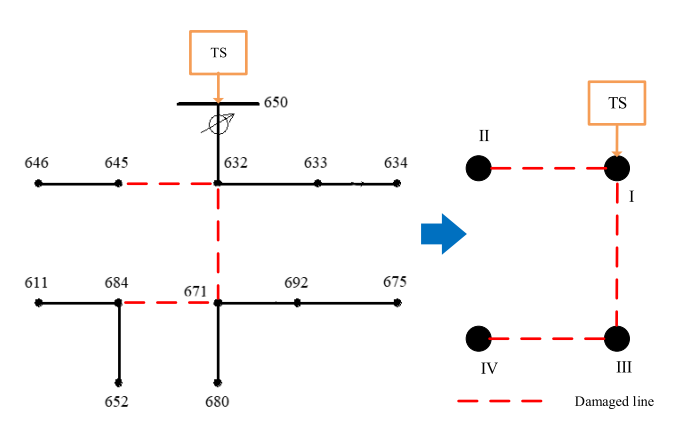


FIGURE 2. Illustration of super-node approximation.

to damages to some feeder lines. Each of these islands is represented by an aggregated node, referred to as a super-node in this paper. All PDA-DERs and loads within an island are aggregated at the corresponding super-node. For example, super-node I contains nodes 650, 632, 633, and 634 and their loads and PDA-DERs. Similarly, super-nodes II, III, and IV represent the other three islands. As a result, the number of nodes considered in the computation is significantly reduced. For example, the IEEE 13-node test feeder with three damaged lines is converted to a network with four super-nodes. Therefore, instead of 13 nodes, four super-nodes are used in the optimization model, which is solved very efficiently, as shown in the next section.

2) THEORETICAL ANALYSIS OF SNA

Remark. The super-node approximation can provide satisfactory accuracy in the context of post-disaster restoration in distribution systems.

To support the statement in the above remark, a mathematical analysis is given as follows:

i. Power losses on feeder lines inside a super-node are minimal and can be ignored in the process of post-disaster restoration since the restoration window is generally short. Therefore, the terms in the DistFlow model that are related to losses can be ignored, which results in the following LinDistFlow model [5], [42]:

L.H.S. of (1p) =
$$\sum_{j} p_{ji,t} + \sum_{k} p_{ik,t}$$
 (4a)

L.H.S. of (1q) =
$$\sum_{j}^{J} q_{ji,t} + \sum_{k}^{\kappa} q_{ik,t}$$
 (4b)

$$v_{i,t} - v_{k,t} - 2(r_{ik}p_{ik,t} + x_{ik}q_{ik,t}) = 0.$$
 (4c)

ii. Voltage difference inside an electrical island is small and can be ignored during restoration. Note that a post-disaster electrical island is a part of a distribution network, which generally consists of fewer nodes. Namely, the electrical distance between any two nodes inside an island or super-node is generally short, with a very small voltage difference. For example, consider nodes 692 and 675 in super-node III from

figure 2. Assume that node 692 is transmitting (40+j30) KVA of power to node 675 at 4.24 KV (1 p.u.). Using system parameters of the IEEE 13-node test feeder, the voltage of node 675 is calculated to be 4.2393 KV, using equations (1d) and (1e). Hence, the voltage difference between nodes 692 and 675 is 0.00069 KV (i.e., 0.0001628 p.u.), which can be ignored during restoration. Therefore, with the voltage difference omitted, constraint (4c) reduces to

$$v_{i,t} - v_{k,t} = 0 (5)$$

where i and $k \in \mathcal{N}_j$ (\mathcal{N}_j is the set of nodes of the jth island). Constraints (4a), (4b), and (5) together imply that all nodes in an island can be aggregated into one single node, i.e., the super-node, provided that the electrical distance between any two nodes is short in a super-node.

D. DISCUSSION ON SNA AND CHR PERFORMANCE

It is worth emphasizing that super-node approximation works very well for severely impacted distribution feeders, where many lines may be damaged, and the number of nodes in a super-node is relatively small. A post-disaster island with many nodes needs to be split into two or multiple super-nodes to preserve the accuracy of the super-node approximation. The MICP formulation of the post-disaster model, in combination with super-node approximation, allocates MERs to post-disaster islands (i.e., super-nodes) rather than individual nodes. To determine the exact locations (nodes) of MERs in a post-disaster island, post-disaster islands' in and out power flows are first determined by applying a combination of CHR and SNA to the whole network. Then, the following MICP optimization model is applied to the individual post-disaster islands by fixing islands' in and out power flows.

Constraints:
$$(1b)-(1d)$$
, $(1f)-(1n)$, $(1p)-(1w)$, (2) , (3) $(6b)$

It is worth noting that if there are line switches or load switches, the decision variables are necessary, and they cannot be merged into one super-node. Therefore, we assume that the loads and distribution lines are not equipped with switches, which is generally true in distribution feeders.

III. CASE STUDY AND RESULTS

This section presents the experimental results of testing the proposed framework and solution methods on IEEE 37-node (Case I) and IEEE 123-node (Case II) test feeders. First, we evaluate the post-disaster restoration model. Second, we compare the computational performance of the proposed solution method with the MINLP model of the post-disaster restoration model. The convex optimization problems were solved by the GUROBI solver via the PYOMO package on a PC with a 64-bit Intel i5 dual-core CPU at 2.50 GHz and 16 GB of RAM, while MINLP problems were solved by the KNITRO solver using NEOS server.



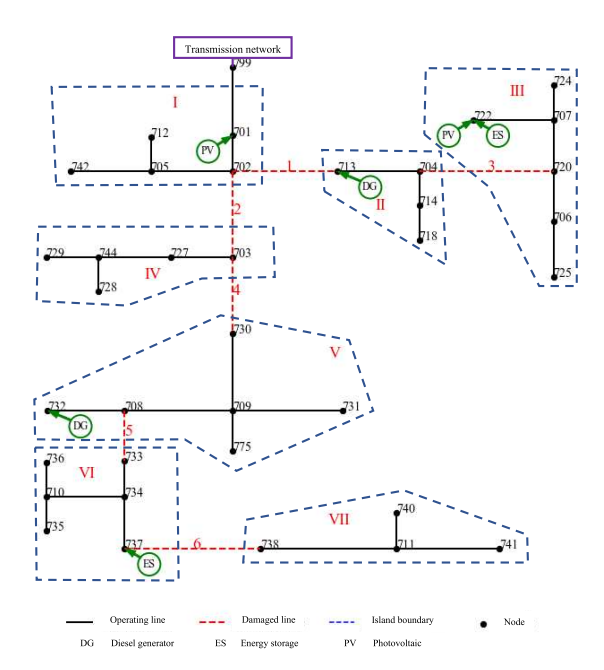


FIGURE 3. Post-disaster distribution feeder (Case I) (DG, ES, and PV refer to SDG, SESS, and SPV, respectively).



FIGURE 4. Post-disaster distribution feeder (Case II) (DG, ES, and PV refer to SDG, SESS, and SPV, respectively).

A. TESTING OF PROPOSED FRAMEWORK: CASE I AND II

The two test feeders are modified by replacing some lines with damaged lines to simulate damages caused by the disaster, as shown in Figure 3 and 4. In the IEEE 37-node test feeder (Case I), six lines are damaged due to disaster, and seven islands are formed. In the IEEE 123-node test feeder (Case II), eight lines are damaged due to disaster, and nine islands are formed. As a matter of fact, such network damage information is available from the damage assessment after a disaster. Note that only PDA-DERs are shown in the Figures 3 and 4. Moreover, DG, ES, and PV refer to

TABLE 1. Available ERRs for Case I and Case II.

	MDGs		MESS	Ss	RCs		
	Size	Units	Size	Units	Capacity	Units	
Case I	1 MW	2			20 hrs	1	
Case I		2			24 hrs	1	
Case II	1 MW	3	1.5MWh/	1	24 hrs		
Case II		3	0.5 MVA	1	∠ 4 III8	2	

TABLE 2. PDA-DERs information (Case I).

SDGs	Capacity	200 KW	200 KW
SDOS	Node #	713	732
SESSs	Capacity	200 KWh/50 KVA	200 KWh/50 KVA
31333	Node #	722	737
SPVs	Capacity	100 KW	100 KW
Sr vs	Node #	701	722

TABLE 3. PDA-DERs information (Case II).

SDGs -	Capacity	100 KW	100 KW	100 KW
	Node #	9	65	87
SESSs	Capacity	100 KWh/25 KVA	100 KWh/25 KVA	100 KWh/25 KVA
3E338 ·	Node #	29	92	113
SPVs -	Capacity	650 KW	650 KW	650 KW
	Node #	19	47	76

TABLE 4. Repair time of damaged lines (Case I & II).

Line #	1	2	3	4	5	6	7	8
Case I (Hrs)	4	6	9	5	8	7		
Case II (Hrs)	5	7	4	4	7	7	4	6

SDG, SESS, and SPV in Figures 3 and 4, respectively. The super-node approximation is applied to both test cases to reduce the dimension of the post-disaster restoration model, which results in seven super-nodes and six damaged lines for the post-disaster IEEE 37-node test feeder (Case I) and nine super-nodes and eight damaged lines for post-disaster IEEE 123-node test feeder (Case II). The post-disaster restoration model in MICP form is then executed. In addition to network damage information, inputs to the post-disaster restoration model are pre-allocated ERRs (Table 1), crew travel times in the network, PDA-DERs information (Tables 2 and 3), and repair times of damaged lines (Table 4). Grid power is assumed to be unavailable for the entire restoration window; however, it can be easily included in the optimization if available. Values of k_1 and k_2 used are -0.8 and 0.8, respectively. Due to a lack of relevant data, crew travel times in the networks were randomly generated in MATLAB, and for brevity, they are omitted in the paper. However, it is noted that the DSOs can choose crew travel times $(TT_{ii,ik})$ and $TT_{i,n}$ for their networks or even set them to zero if the geographical area of the network is relatively small.

The post-disaster restoration model was executed to determine 1) the optimal locations of MERs and 2) the



TABLE 5. Optimal locations of MERs (Case I & II).

		Case I	Case II			
	Super-nod	Super-node (actual node)				
MDGs	I (701)	VI (737)	IV (48)	V (56)	VI (76)	
MESSs				III (28)		

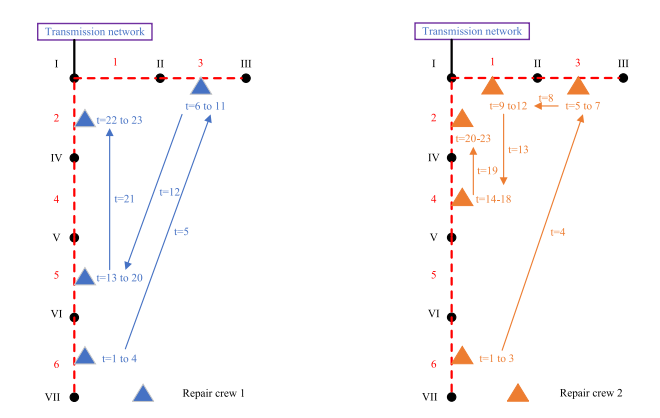


FIGURE 5. Routing and repair schedule of RCs-Case I.

optimal repair order of damaged lines by RCs. The locations of MERs were optimally fixed for the entire restoration window by enforcing the constraint (1t). As such, the optimal locations of MERs for Case I and II, obtained from the post-disaster restoration model, are given in Table 5. It is observed that the optimal locations of two MDGs are super-node I (node 701) and super-node VI (node 737) in Case I. The exact locations (node 701 and node 737) were obtained by applying the post-disaster restoration model (6) to super-node I and VI separately by fixing the in-flow and out-flow of the super-nodes. The routing of RCs to repair damaged lines is provided in Figure 5 for Case I and Figure 6 for Case II with a time resolution of one hour. As seen from Figure 5, RC-1 and RC-2 start repairing damaged line 6 first in Case I. It is noted that two RCs were allowed to work on the same line at a time. After repairing damaged line 6 for four consecutive hours, RC-1 travels to damaged line $3 (6 \rightarrow 3)$ in period 5. Accordingly, RCs travel to repair damaged lines 3, 1, 5, 4, 2 in the order. Similarly, as seen from Figure 6, RC-1 starts repairing damaged line 7, and RC-2 starts repairing damaged line 3 first in Case II. As such, RCs travel to repair damaged lines 1, 2, 8, 6, 5, 4 in the order. The obtained locations of MERs and the routing schedule of RCs are the optimal solutions for achieving the minimum energy not served for the entire restoration window. The bar charts of the total energy required (TER) and the total energy supplied (TES) for each period are provided in Figures 7 and 8 for Case I and Case II, respectively, with a time resolution of four hours. The difference between TER and TES is unserved energy. It is worth noting that unserved energy gets smaller and smaller when more and more damaged lines are repaired. The repair of damaged lines is impacted by various systemspecific parameters, amount and locations of PDA-DERs, amount of ERRs, and repair times of damaged lines.

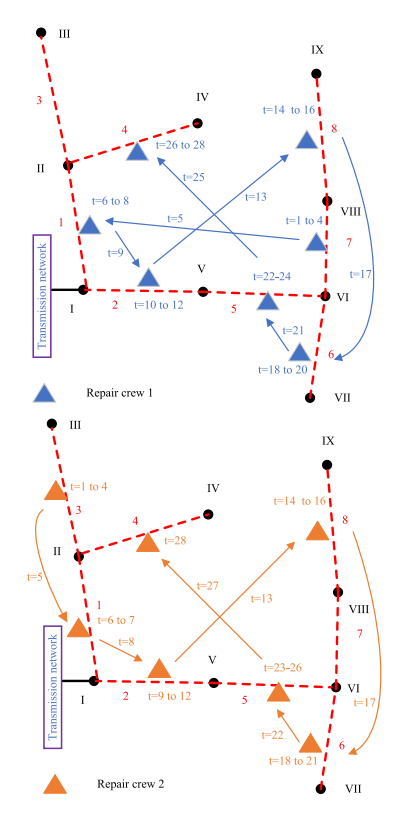


FIGURE 6. Routing and repair schedule of RCs-Case II.

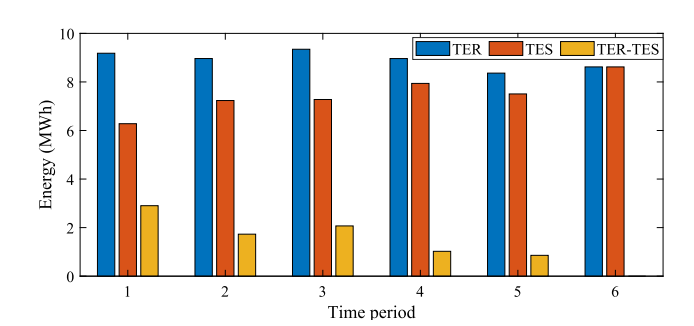


FIGURE 7. TER vs TES vs TER-TS for Case I.

B. COMPUTATIONAL PERFORMANCE OF PROPOSED SOLUTION METHOD

In this subsection, the computational performance of the proposed solution approaches, i.e., convex hull relaxation (CHR) and super-node approximation (SNA), was compared individually and jointly with the non-linear and linear forms of the problem, as shown in Table 6. In the table, *MINLP* refers to the MINLP form of the post-disaster restoration model without using CHR and SNA. Similarly, *SNA* refers to the MINLP form of the model with only SNA. *CHR* refers to the convex form of the model, but without SNA. *SNA+CHR* refers to the convex form of the model with SNA. Moreover, *Lin* refers to the restoration model with linear DistFlow for power flow but without SNA. *Lin+SNA* refers to the restoration model with linear DistFlow for power flow and SNA. It is worth noting that the linear model



		MINLP	SNA	CHR	SNA+CHR	Lin	SNA+Lin
Case I -	Objective value	N/A	N/A	8.59 MWh	8.58 MWh	8.58 MWh	8.58 MWh
	Time	>8h	>8h	≈4h	≈2m	≈3h	≈3m
Case II	Objective value	N/A	N/A	9.61 MWh	9.59 MWh	9.59 MWh	9.58 MWh
	Time	>8h	>8h	>8h	≈10m	>8h	≈6m

TABLE 6. Computational performance of proposed solution approach.

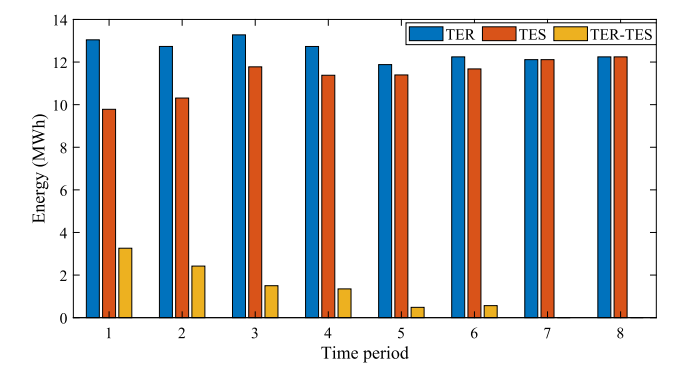


FIGURE 8. TER vs TES vs TER-TS for Case II.

of constraint (10) is not available; therefore, convex hull relaxation of (10) is used in *Lin* and *Lin+SNA* in the Table. The NEOS server [48] could not solve MINLP and SNA forms of the model, citing that computation exceeded the time limit of 8 hours, which indicates that the MINLP form of the model is computationally intractable. CHR form of the model in Case I was solved in approximately 4 hours, while it took more than 8 hours in Case II. Similarly, Lin form of the model in Case I was solved in approximately 3 hours, while it took more than 8 hours in Case II. However, the SNA+CHR form of the model took approximately 2 minutes and 10 minutes for Case I and II, respectively. Similarly, the SNA+Lin form of the model took approximately 3 minutes and 6 minutes for Case I and II, respectively. It is seen from the Table that convex and linear forms of the model alone (without SNA) do not achieve the computational efficiency desired. In Case I, SNA+CHR is the most computationally efficient, while the SNA+Lin is the most efficient in Case II. Note that SNA+CHR and SNA+Lin forms have similar objective values as other models; however, the SNA+CHR and SNA+Lin forms of the model for both Case I and II were solved remarkably efficiently.

IV. CONCLUSION

In this paper, we proposed a computationally tractable approach for the restoration of the distribution systems coordinating ERRs and PDA-DERs after a disaster. In the proposed post-disaster restoration model, pre-allocated ERRs and PDA-DERs are co-optimized to minimize the unserved energy, obtaining the optimal routing of repair crews to repair damaged distribution lines. The proposed approach is technically more feasible and tractable since the proposed post-disaster model in MINLP form is convexified using con-

vex hull relaxation. Besides, the super-node approximation is introduced to efficiently solve the MICP model for larger test feeders. The proposed framework and solution methods are tested using the IEEE 37 and 123 node test feeders. The test results indicate the successful post-disaster allocation of ERRs in coordination with PDA-DERs for the disaster-resilient restoration of the distribution system. Even though the proposed framework and models are more suitable for high-wind events such as cyclones, hurricanes, and tornadoes, they can be easily extended to include other disastrous events such as snowstorms and earthquakes in future research.

REFERENCES

- P. Hines, J. Apt, and S. Talukdar, "Trends in the history of large blackouts in the United States," in *Proc. IEEE Power Energy Soc. Gen. Meeting Convers. Del. Electr. Energy 21st Century*, Jul. 2008, pp. 1–8.
- [2] Executive Office of the President, The White House, Council of Economic Advisers, Economic Benefits of Increasing Electric Grid Resilience to Weather Outages, The Council, Washington, DC, USA, 2013.
- [3] A. B. Smith and R. W. Katz, "U.S. billion-dollar weather and climate disasters: Data sources, trends, accuracy and biases," *Natural Hazards*, vol. 67, no. 2, pp. 387–410, Jun. 2013.
- [4] Presidential Policy Directive-Critical Infrastructure Security and Resilience, Press Release, White House, Washington, DC, USA, Feb. 2013.
- [5] Q. Li, R. Ayyanar, and V. Vittal, "Convex optimization for des planning and operation in radial distribution systems with high penetration of photovoltaic resources," *IEEE Trans. Sustain. Energy*, vol. 7, no. 3, pp. 985–995, Jul. 2016.
- [6] C. L. Moreira, F. O. Resende, and J. A. P. Lopes, "Using low voltage MicroGrids for service restoration," *IEEE Trans. Power Syst.*, vol. 22, no. 1, pp. 395–403, Feb. 2007.
- [7] J. Li, X.-Y. Ma, C.-C. Liu, and K. P. Schneider, "Distribution system restoration with microgrids using spanning tree search," *IEEE Trans. Power Syst.*, vol. 29, no. 6, pp. 3021–3029, Nov. 2014.
- [8] M. Nemati, M. Braun, and S. Tenbohlen, "Optimization of unit commitment and economic dispatch in microgrids based on genetic algorithm and mixed integer linear programming," *Appl. Energy*, vol. 210, pp. 944–963, Jan. 2018.
- [9] F. Wang, C. Chen, C. Li, Y. Cao, Y. Li, B. Zhou, and X. Dong, "A multistage restoration method for medium-voltage distribution system with DGs," *IEEE Trans. Smart Grid*, vol. 8, no. 6, pp. 2627–2636, Nov. 2017.
- [10] H. Ji, C. Wang, P. Li, G. Song, H. Yu, and J. Wu, "Quantified analysis method for operational flexibility of active distribution networks with high penetration of distributed generators," *Appl. Energy*, vol. 239, pp. 706–714, Apr. 2019.
- [11] Z. Wang, J. Wang, and C. Chen, "A three-phase microgrid restoration model considering unbalanced operation of distributed generation," *IEEE Trans. Smart Grid*, vol. 9, no. 4, pp. 3594–3604, Jul. 2018.
- [12] Y.-J. Kim, J. Wang, and X. Lu, "A framework for load service restoration using dynamic change in boundaries of advanced microgrids with synchronous-machine DGs," *IEEE Trans. Smart Grid*, vol. 9, no. 4, pp. 3676–3690, Jul. 2018.
- [13] B. Chen, C. Chen, J. Wang, and K. L. Butler-Purry, "Multi-time step service restoration for advanced distribution systems and microgrids," *IEEE Trans. Smart Grid*, vol. 9, no. 6, pp. 6793–6805, Nov. 2018.
- [14] Y. Xu, C.-C. Liu, Z. Wang, K. Mo, K. P. Schneider, F. K. Tuffner, and D. T. Ton, "DGs for service restoration to critical loads in a secondary network," *IEEE Trans. Smart Grid*, vol. 10, no. 1, pp. 435–447, Jan. 2019.



- [15] S. Poudel and A. Dubey, "Critical load restoration using distributed energy resources for resilient power distribution system," *IEEE Trans. Power Syst.*, vol. 34, no. 1, pp. 52–63, Jan. 2019.
- [16] B. Chen, Z. Ye, C. Chen, and J. Wang, "Toward a MILP modeling framework for distribution system restoration," *IEEE Trans. Power Syst.*, vol. 34, no. 3, pp. 1749–1760, May 2019.
- [17] F. Resende, N. J. Gil, and J. Lopes, "Service restoration on distribution systems using multi-microgrids," *Eur. Trans. Electr. Power*, vol. 21, no. 2, pp. 1327–1342, 2011.
- [18] C. Chen, J. Wang, F. Qiu, and D. Zhao, "Resilient distribution system by microgrids formation after natural disasters," *IEEE Trans. Smart Grid*, vol. 7, no. 2, pp. 958–966, Mar. 2016.
- [19] Y. Zhao, J. Lin, Y. Song, and Y. Xu, "A hierarchical strategy for restorative self-healing of hydrogen-penetrated distribution systems considering energy sharing via mobile resources," *IEEE Trans. Power Syst.*, vol. 38, no. 2, pp. 1388–1404, Mar. 2023.
- [20] C. Wang, G. Song, P. Li, H. Ji, J. Zhao, and J. Wu, "Optimal siting and sizing of soft open points in active electrical distribution networks," *Appl. Energy*, vol. 189, pp. 301–309, Mar. 2017.
- [21] S. Lei, J. Wang, C. Chen, and Y. Hou, "Mobile emergency generator pre-positioning and real-time allocation for resilient response to natural disasters," *IEEE Trans. Smart Grid*, vol. 9, no. 3, pp. 2030–2041, May 2018.
- [22] J. Kim and Y. Dvorkin, "Enhancing distribution system resilience with mobile energy storage and microgrids," *IEEE Trans. Smart Grid*, vol. 10, no. 5, pp. 4996–5006, Sep. 2019.
- [23] L. Che and M. Shahidehpour, "Adaptive formation of microgrids with mobile emergency resources for critical service restoration in extreme conditions," *IEEE Trans. Power Syst.*, vol. 34, no. 1, pp. 742–753, Jan. 2019.
- [24] S. Lei, C. Chen, H. Zhou, and Y. Hou, "Routing and scheduling of mobile power sources for distribution system resilience enhancement," *IEEE Trans. Smart Grid*, vol. 10, no. 5, pp. 5650–5662, Sep. 2019.
- [25] S. Lei, C. Chen, Y. Li, and Y. Hou, "Resilient disaster recovery logistics of distribution systems: Co-optimize service restoration with repair crew and mobile power source dispatch," *IEEE Trans. Smart Grid*, vol. 10, no. 6, pp. 6187–6202, Nov. 2019.
- [26] G. Zhang, F. Zhang, X. Zhang, Z. Wang, K. Meng, and Z. Y. Dong, "Mobile emergency generator planning in resilient distribution systems: A three-stage stochastic model with nonanticipativity constraints," *IEEE Trans. Smart Grid*, vol. 11, no. 6, pp. 4847–4859, Nov. 2020.
- [27] B. Taheri, A. Safdarian, M. Moeini-Aghtaie, and M. Lehtonen, "Distribution system resilience enhancement via mobile emergency generators," *IEEE Trans. Power Del.*, vol. 36, no. 4, pp. 2308–2319, Aug. 2021.
- [28] Z. Yang, A. Martí, Y. Chen, and J. R. Martí, "Optimal resource allocation to enhance power grid resilience against hurricanes," *IEEE Trans. Power Syst.*, vol. 38, no. 3, pp. 2621–2629, May 2023.
- [29] S. Yao, P. Wang, X. Liu, H. Zhang, and T. Zhao, "Rolling optimization of mobile energy storage fleets for resilient service restoration," *IEEE Trans. Smart Grid*, vol. 11, no. 2, pp. 1030–1043, Mar. 2020.
- [30] W. Wang, X. Xiong, C. Xiao, and B. Wei, "A novel mobility model to support the routing of mobile energy resources," *IEEE Trans. Smart Grid*, vol. 13, no. 4, pp. 2675–2678, Jul. 2022.
- [31] W. Wang, Y. He, X. Xiong, and H. Chen, "Robust survivability-oriented scheduling of separable mobile energy storage and demand response for isolated distribution systems," *IEEE Trans. Power Del.*, vol. 37, no. 5, pp. 3521–3535, Oct. 2022.
- [32] Z. Yang, P. Dehghanian, and M. Nazemi, "Seismic-resilient electric power distribution systems: Harnessing the mobility of power sources," *IEEE Trans. Ind. Appl.*, vol. 56, no. 3, pp. 2304–2313, May 2020.
- [33] X. Jiang, J. Chen, W. Zhang, Q. Wu, Y. Zhang, and J. Liu, "Two-step optimal allocation of stationary and mobile energy storage systems in resilient distribution networks," J. Modern Power Syst. Clean Energy, vol. 9, no. 4, pp. 788–799, Jul. 2021.
- [34] Y. Wang, D. Qiu, F. Teng, and G. Strbac, "Towards microgrid resilience enhancement via mobile power sources and repair crews: A multi-agent reinforcement learning approach," *IEEE Trans. Power Syst.*, vol. 39, no. 1, pp. 1–17, 2023.
- [35] W. Wang, X. Xiong, Y. He, J. Hu, and H. Chen, "Scheduling of separable mobile energy storage systems with mobile generators and fuel tankers to boost distribution system resilience," *IEEE Trans. Smart Grid*, vol. 13, no. 1, pp. 443–457, Jan. 2022.

- [36] Z. Zhao, F. Luo, J. Zhu, and G. Ranzi, "Multi-stage mobile BESS operational framework to residential customers in planned outages," *IEEE Trans. Smart Grid*, vol. 14, no. 5, pp. 3640–3653, Jul. 2023.
- [37] Q. Sui, F. Wei, C. Wu, X. Lin, and Z. Li, "Self-sustaining of post-disaster pelagic island energy systems with mobile multi-energy storages," *IEEE Trans. Smart Grid*, vol. 14, no. 4, pp. 2645–2655, Jun. 2023.
- [38] Z. Ye, C. Chen, B. Chen, and K. Wu, "Resilient service restoration for unbalanced distribution systems with distributed energy resources by leveraging mobile generators," *IEEE Trans. Ind. Informat.*, vol. 17, no. 2, pp. 1386–1396, Feb. 2021.
- [39] M. Nazemi, P. Dehghanian, X. Lu, and C. Chen, "Uncertainty-aware deployment of mobile energy storage systems for distribution grid resilience," *IEEE Trans. Smart Grid*, vol. 12, no. 4, pp. 3200–3214, Jul. 2021.
- [40] M. Yan, M. Shahidehpour, A. Paaso, L. Zhang, A. Alabdulwahab, and A. Abusorrah, "Distribution system resilience in ice storms by optimal routing of mobile devices on congested roads," *IEEE Trans. Smart Grid*, vol. 12, no. 2, pp. 1314–1328, Mar. 2021.
- [41] S. Sharma, Q. Huang, A. Tbaileh, and Q. Li, "Scenario-based analysis for disaster-resilient restoration of distribution systems," in *Proc. North Amer. Power Symp. (NAPS)*, Oct. 2019, pp. 1–6.
- [42] M. E. Baran and F. F. Wu, "Optimal capacitor placement on radial distribution systems," *IEEE Trans. Power Del.*, vol. 4, no. 1, pp. 725–734, 1989.
- [43] Q. Li and V. Vittal, "Convex hull of the quadratic branch AC power flow equations and its application in radial distribution networks," *IEEE Trans. Power Syst.*, vol. 33, no. 1, pp. 839–850, Jan. 2018.
- [44] S. Lei, C. Chen, Y. Song, and Y. Hou, "Radiality constraints for resilient reconfiguration of distribution systems: Formulation and application to microgrid formation," *IEEE Trans. Smart Grid*, vol. 11, no. 5, pp. 3944–3956, Sep. 2020.
- [45] Q. Li, S. Yu, A. S. Al-Sumaiti, and K. Turitsyn, "Micro water-energy nexus: Optimal demand-side management and quasi-convex hull relaxation," *IEEE Trans. Control Netw. Syst.*, vol. 6, no. 4, pp. 1313–1322, Dec. 2019.
- [46] A. Ulusan and O. Ergun, "Restoration of services in disrupted infrastructure systems: A network science approach," *PLoS ONE*, vol. 13, no. 2, Feb. 2018, Art. no. e0192272.
- [47] D. S. Hirschberg, A. K. Chandra, and D. V. Sarwate, "Computing connected components on parallel computers," *Commun. ACM*, vol. 22, no. 8, pp. 461–464, Aug. 1979.
- [48] J. Czyzyk, M. P. Mesnier, and J. J. More, "The NEOS server," *IEEE Comput. Sci. Eng.*, vol. 5, no. 3, pp. 68–75, Jul. 1998.



SANTOSH SHARMA (Graduate Student Member, IEEE) received the Bachelor of Engineering degree in electrical engineering from Tribhuvan University, Kathmandu, Nepal, in 2016. He is currently pursuing the Ph.D. degree in electrical engineering with the University of Central Florida. His research interests include the coordination of interdependent critical infrastructures, such as power systems, water delivery systems, and transportation networks in normal and emergency conditions.



QIFENG LI (Senior Member, IEEE) received the Ph.D. degree in electrical engineering from Arizona State University, Tempe, AZ, USA, in 2016. He is currently an Assistant Professor with the Department of Electrical and Computer Engineering, University of Central Florida (UCF), Orlando, FL, USA. Before joining the UCF Faculty, he held a position of a Postdoctoral Associate with the Department of Mechanical Engineering, Massachusetts Institute of Technology (MIT),

Cambridge, MA, USA, from 2016 to 2018. His research interests include convex optimization, uncertainty-aware optimization, and nonlinear systems with applications in power and energy systems.